Title
DIRECT DISLOCATION VELOCITY MEASUREMENT IN SILICON BY X-RAY TOPOGRAPHY

Authors
Kannan, V.C.
Washburn, J.

Publication Date
1969-09-01

Submitted to J. Chemical Physics

UCRL-18866
Preprint

DIRECT DISLOCATION VELOCITY MEASUREMENT IN SILICON BY X-RAY TOPOGRAPHY

V. C. Kannan and J. Washburn

September 1969

AEC Contract No. W-7405-eng-48

LAWRENCE RADIATION LABORATORY
UNIVERSITY of CALIFORNIA BERKELEY

UCRL-18866

DISCLAIMER

UCRL-18866

DIRECT DISLOCATION VELOCITY MEASUREMENT IN SILICON BY X-RAY TOPOGRAPHY

V. C. Kannan and J. Washburn

Inorganic Materials Research Division, Lawrence Radiation Laboratory, Department of Materials Science and Engineering, College of Engineering, University of California, Berkeley, California

ABSTRACT

Glide velocity measurements were made on isolated screw and 60° dislocations in silicon for the temperature range 775°C to 925°C. The X-ray topographs which were used to reveal dislocation displacements also gave qualitative information concerning the early stages of dislocation multiplication in higly perfect silicon crystals.

Freshly generated dislocations were more mobile than aged dislocations. Pinning points which were tentatively attributed to thermal jogs developed along the lines. The pinning point spacing decreased with increasing temperature as would be expected for a jog formation energy of 1.2 ev. Heating to above 1000°C effectively immobilized all the dislocations present in the crystal. On subsequent loading at 825°C, no motion took place until the stress was high enough to cause catastrophic multiplication when a segment of dislocation did break away. This resulted in the formation of heavy bands of slip.

For fresh dislocations in the temperature range studied the drag of jogs did not appear to be rate controlling because the jog concentration was too small. The temperature dependence of velocity was analyzed on the basis of a kink pair nucleation and kink propagation model. The measured activation energy for motion of both 60° and screw dislocations was $1.8 \pm .3$ ev.

I. INTRODUCTION

Measurements of velocities of individual dislocations are of particular interest for further development of the theories of the flow stress, solution hardening, creep and other plastic properties of pure and slightly impure single crystals. Gilman and Johnston[1] were the first to develop an etch-pitting technique for the measurement of dislocation velocities in LiF. Shortly thereafter, by employing this technique with slight modifications, speeds of individual dislocations were measured in a number of crystals by various authors.[2-10] A striking observation common to all these investigations was that dislocations did not move uniformly in the crystal. Even neighboring dislocations having the same Burger's vector often moved with widely different speeds. As a result, every recorded value of dislocation velocity by these authors is an average of 40 to 100 dislocations that moved various distances under the same applied stress pulse. Therefore, the true meaning of this seemingly fundamental data on the stress dependence of dislocation velocity becomes unclear because the characteristics of the moving dislocations are not well known. For example, jogs on a moving screw dislocation must be dragged non-conservatively and even on edge-dislocations jogs greatly reduce mobility. This dragging force on the moving dislocation is dependent on the jog density and the heights of the jogs, but very little quantitative information on this is available. Qualitative observations by Young and Sherrill[11] and by Petroff and Washburn[12] in copper have shown that heavily jogged dislocations do require higher stresses for motion than do the relatively jog-free dislocations. Therefore, data on dislocation velocities at various temperatures and applied stresses can only be interpreted unambiguously if the moving dislocation can be well

characterized. Parameters such as orientation, radius of curvature and jog density must be known. Obviously, it is not experimentally possible to obtain quantitative information on dislocation velocity as affected by the above factors from a single technique, but X-ray topography is a powerful tool for the direct observation of mobilities of isolated dislocations in nearly perfect crystals. Measurements of positions of individual dislocations made repeatedly after motion at different temperatures and applied stresses can give information on glide velocity and at the same time help to characterize the moving dislocation. Because it is possible to observe long segments of dislocation line by the X-ray technique, some of its characteristics, i.e., edge, screw, straight or curved, can be correlated with its velocity data. This is an important advantage over the simpler etch-pit technique because the latter can not give any information regarding the characteristics of the moving dislocation. Another advantage of the X-ray technique is that true displacement can be calculated. For the etch-pit technique, the distance moved by the dislocation, perpendicular to to itself, is equal to the pit displacement only when the dislocation intersects the trace of the glide plane on the surface of observation at right angles and there is no way to know this angle of intersection. The primary limitation of the X-ray technique is its poor resolution which is only of the order of 4μ. Therefore, the fine scale configuration of a dislocation line can not be revealed.

In the present investigation, the Lang X-ray technique was employed to study the motion of isolated individual dislocations in highly perfect silicon single crystals. In crystals with diamond cubic structure, dislocations are immobile at room temperature. They become mobile gradually above about

0.5 Tm where Tm is the temperature of melting. This is an important experimental advantage because by simply cooling under load, any dislocation configuration can be frozen in place for observation at room temperature. The speeds of dislocations in these crystals vary slowly with the applied stress;[13] for example, roughly as σ^2 to $\sigma^{1.5}$ at higher stress levels and $\sigma^{3.5}$ at lower stress levels. This dependence can be contrasted with σ^{25} and σ^{44} measured for LiF and silicon-iron respectively.[14] Therefore it is experimentally easier to control the velocities of dislocations in silicon as compared to metals.

The main purpose of the present investigation was to observe the controlled motion of individual well isolated dislocations under small applied stresses near .5 Tm and to correlate this mobility data with the appearance of the dislocation lines, i.e., straight, wavy or curved, edge or screw. In the course of the experiment, it was also hoped to obtain qualitative information on the motion of dislocations at higher temperatures and on the multiplication and distribution of dislocations during the early stages of deformation of highly perfect silicon single crystals.

II. EXPERIMENTAL PROCEDURE

The initial dislocation density in all the specimens was zero within the limits of experimental observation. Therefore, as a first step, fresh dislocations had to be introduced before their motion could be studied. In one set of experiments, dislocations were introduced by pressing a molybdenum pointer on the specimen surface at about 1000° - 1050°C. Dislocations were generated at the point of compression and traveled long distances into the specimen. This provided qualitative information on dislocation motion and multiplication at ∿1000°C. In the second set of experiments, quantitative data on dislocation velocity was obtained by measuring the displacement of isolated individual dislocations caused by application of a tensile stress pulse. The loading was carried out either in vacuum of 10^{-6} mm Hg or in an atmosphere of high purity helium.

Silicon single crystals were obtained from the Texas Instruments Co. in the form of cylindrical rods of 1 inch diameter X 6 inches long. The crystals were Czochralski grown, N-type and had a residual resistivity of ∿50Ω-cm. Wafers of 45 mil thickness with desired orientation were cut from the original cylinder with a diamond wheel. In order to remove the surface damage introduced while cutting, the wafers were chemically polished. The final thickness of the wafers varied from 1.0 to 1.1 mm.

Tensile specimens of desired orientation were cut from the wafers in an ultrasonic cutting machine. A special molybdenum jig was employed to grip the specimens. Dead loading was employed for stress pulses ranging from ten minutes to one hour. The temperature of the specimens was regulated within ± 5°C of the desired test temperature and the recorded temperature was within ± 1°C. After the test, the specimens were cooled

rapidly to room temperature in vacuum and under load.

After testing, the X-ray images of the specimens were photographed using the Lang technique with $MoK\alpha_1$ - radiation. 2.5 x 3.5 cm Illford G-plates with 50μ emulsion thickness were used. Each plate needed an exposure time of 20 minutes/mm. The photographic plates were processed using a special developing procedure to obtain the best contrast.[15] Other details of the experimental procedure are described in Ref. 16.

Topographs were taken before and after loading the specimen at a particular temperature for a specified length of time. The distance traveled by the dislocations was measured as follows. The areas in the vicinity of the dislocation in question were examined to locate corresponding reference points on the two topographs. Small black-dots due to surface imperfections or markings frequently served this purpose. The distance moved on the glide plane perpendicular to the dislocation line was computed by measuring its distance from the reference dots before and after testing. Knowing the duration of load-application, the average velocity of the dislocation was calculated.

All measurements were made on the final prints taking particular care to correct for any small differences in magnification. Only nominal magnifications are quoted in the figure captions.

III. EXPERIMENTAL RESULTS

A. Propagation of Dislocations at High Temperatures

Fig. 1 shows groups of dislocations generated by pressing a molybdenum pointer on the specimen surface at about 1000°C for ∿15 minutes. Of particular interest in this topograph are the dislocation lines at A ($b = \frac{a}{2}[\bar{1}01]$) that developed small pinning points, cusps, long cusps and well-developed helical segments as they traveled in the crystal. Fig. 2a is a topograph of a tensile specimen which was pulled at 850°C for 30 minutes under a tensile stress of ∿200 gm/mm^2. No existing dislocations moved nor were any generated. The specimen was then pulled again at 950°C under a small tensile stress (∿20 gm/mm^2). Fig. 2(b) shows that some dislocations moved out to the specimen surface in the area B. When the specimen was once again loaded to a stress of 380 gm/mm^2 at 900°C, Fig. 2(c), profuse generation of dislocations occured originating from the edges of the specimen, but the original high temperature dislocations still did not move. Similarly, a specimen with zero initial dislocation density was loaded to a tensile stress of ∿180 gm/mm^2 at 950°C. The dislocations generated under these conditions are shown in Fig. 3(a). Again, all the dislocations were generated from the side surfaces. Dislocations, $b = \frac{a}{2}[\bar{1}10]$, in the area A have developed pinning points during their motion. On close observation, even the nearly straight dislocations reveal pinning points along their length as in area B. The specimen was then pulled again at 850°C under a resolved shear stress of 36 gm/mm^2 and the topograph of Fig. 3(b) was taken. The final topograph of the series shows intense dislocation multiplication which apparently occured as a result of the movement of the curved dislocation segments at area A in Fig. 3(a). The individual lines in the resulting slip bands are

not resolved since the density was too high (probably of the order of 10^6 dislocations/cm^2. Electron microscopy was used to study the arrangement of dislocations within the bands. A few specimens were loaded to a tensile stress of $\sim$200 gm/mm^2 along [110] at 920°C - 950°C for 20 minutes to introduce dislocations of a density $\sim 10^4 - 10^5$ dislocations/cm^2. [The X-ray topograph of Fig. 3(c) corresponds approximately to this amount of deformation]. Electron micrographs of foils obtained from these specimens are shown in Fig. 4(a) and (b). The observed dislocations were mostly edge dislocation dipoles and elongated loops of varying lengths and widths. The dislocation distribution was highly inhomogeneous. Large areas were completely free of dislocations while clusters of entangled dislocations were found at other areas on the primary slip plane. Many dislocations were smoothly curved even at this magnification ($\sim$20,000X) while others were accurately straight. Dislocation dissociation was not observed even at the nodes.

B. Motion of Individual Dislocations and Measurement of Dislocation Velocities

Fig. 5 is an enlargement of topographs made before and after tensile loading at 825°C to a resolved shear stress of 36 gm/mm^2. The geometry of the specimen and the loading direction are shown on the topograph itself. The velocities of screw and 60° - segments of many comparatively isolated dislocations were measured and are listed in Table I. In the final column are given the characteristics of the dislocation line, namely whether the dislocation was straight, wavy or curved within the limits of the resolution of the X-ray topographs. If the distance traveled by a dislocation segment is approximately the same at all points along its length the motion has been

referred to as uniform. "Irregular motion" indicates that the segment became increasingly wavy or curved. Dislocation segments lying at the head of an inverse pile-up (Nos. 12, 13, 14, 15, 16) moved at higher velocities as might be expected. Also, isolated 60° segments moved 2 1/2 to 3 times faster than the screw segments. Straight dislocations, generally moved at higher speeds than curved ones (compare the dislocations 11 and 20 with 5 and 17). Conversely, dislocations moving at higher speeds tended to remain straight, while slow-moving dislocations generally became wavy or curved. Figure 6(a) and (b) contain the topographs of another specimen pulled in tension under the same resolved shear stress of 36 gm/mm^2 but at 850°C. The various dislocations are labelled and the data is listed in Table II. Again, the speeds of 60° dislocations were higher than that of the screw segments by a factor of ~ 4. Of particular interest in this specimen is dislocation No. 1 that became wavy during its motion. The motion of dislocations 4, 5, 6, 7, and 8 were highly inhomogeneous. Consequently, it was difficult to define their velocities. The 60° - segments at the head of the group, Nos. 13 and 14, traveled much longer distances than did the isolated segments. These high speed segments also remained straight after moving. Velocities were also measured at 775°, 900°, and 920°C and the data are displayed in Fig. 7 for screw and 60° dislocations.

IV. DISCUSSION

A. Propagation of Dislocations at High Temperatures

The present work shows that dislocations near screw orientation acquired pinning points, trailing dipoles and even helical segments as they moved in the crystal at 1000°C. One can identify all these features on the moving dislocation lines in Fig. 1. This can be explained by assuming that moving screw dislocations continuously develop jogs at high temperatures.[17] On a long screw dislocation which has jogs of varying heights along its length continued motion will result in the formation of a dipole wherever there is a jog at least several Burger's vectors high; unit jogs can be dragged along leaving behind a trail of vacancies or interstitials depending upon the sign of the jog. If the jog height exceeds a critical length given approximately by:

$$h = \frac{\mu b}{8\,\pi(1-\nu)\,\tau} \qquad (1)$$

where τ is the shear-stress acting on the dislocation line, μ is the elastic shear modulus, ν is Poissons ratio and b is the Burger's vector, then the two edge segments of the dipole will be driven past each other in opposite directions by the applied stress. This constitutes multiplication.

Although jogs large enough to result in dipole trails have been observed on moving screw dislocations by many investigators, it is not clearly established exactly how they are formed. Jogs can be formed by a number of mechanisms. An obvious process is intersection of two dislocations resulting in either acquisition of a jog by both dislocations or a jog by one and a kink by the other. A moving screw dislocation can acquire multiple jogs if it cuts a grown-in small angle twist boundary or any group of dislocations of like sign.

Double cross-slip and climb can also lead to jog formation under certain conditions. Impurity clusters, fine precipitates or voids may cause local double cross-slip. It is extremely difficult to know which of these mechanisms are important in a particular case.

In the present work, the intersection mechanism can be ruled out because the crystals were dislocation free and there were no small angle boundaries or grown-in dislocation networks. Similarly, there was no evidence for the presence of impurity clusters or precipitates.

It is proposed that climb of a short segment of dislocation which is near screw orientation could lead to formation of long jogs in the following way. Consider a long screw dislocation on the primary glide plane that is pinned at its ends by small dipoles. When the dislocation attempts to move, the segment between the pinning points bows out. The mid-point of the bowed segment is exactly in screw orientation, but the segments just to the left and right of the mid-point have some edge character. If the edge component at the left of the mid-point has its associated extra half plane of atoms above the glide plane, then that on the right has it below. If excess vacancies around the dislocation induce climb of these edge components, the left and right sides will climb in opposite directions. Any additional movement of the dislocation is then accompanied either by dragging of the new jogs non-conservatively or their glide. If some become trapped on the pure screw part of the segment then a new dipole will be initiated. The spacing of the dipole can subsequently increase as the moving dislocation absorbs more vacancies while sweeping along the glide plane. These vacancies could arrive at the dipole by diffusing along the dislocation line (pipe-diffusion), or new jogs can be formed which glide into the dipole.

Vacancies in excess of the equilibrium concentration will be present in the crystal due to dragging of elementary jogs non-conservatively by moving dislocations. Voids and vacancy clusters may also be left in the crystal during the growth of the crystal from the liquid state. Voids in silicon samples grown in a hydrogen atmosphere have been reported by Yukimoto.[18] Vacancies can also be trapped particularly in dislocation free crystals while cooling from high temperature.

The experimental results described previously have also shown that dislocations generated at high temperatures (~1000°C) or exposed to high temperatures, become immobile at lower temperatures (~850°C) even under loads high enough to generate and move fresh dislocations. It is possible that they are immobilized during aging by becoming heavily jogged during climb. It is not possible to ascertain from the present investigation whether or not dislocations were also locked during aging by impurities or impurity clusters. Impurities might also contribute to jog formation by promoting cross-slip. Such a mechanism has been originally put forward by Johnston[19] to account for the dragging stresses of screw dislocations due to the presence of small amounts of impurities. The existing experimental data is still too sparse to confirm which of these mechanisms is important. Unfortunately, it is not likely that X-ray topography can contribute directly to answering these questions because of its limited resolving power.

The present electron microscope results on the nature of dislocations in silicon lend support to similar observations made on deformed germanium by Alexander and Haasen.[20]

The localization of deformation into narrow regions on the primary slip plane can only be explained by an avalanche-like multiplication at dislocation sources. The dipole formation mechanism proposed by Washburn[17] and

dipole sources of the type observed in silicon-iron by Low and Turkalo[21] could explain the present observations.

B. Mobilities of Individual Dislocations

The pinning points on the dislocation lines must be associated either with vacancy clusters and impurities or with thermal jogs. The present experimental observations suggest thermal jog-pinning. For example, it was observed that the pinning points were quite uniformly distributed along the entire length of the dislocation lines. Also, the average pinning distance decreased with increasing temperature.

Following Friedel,[22] the equilibrium length ℓ_j between unit jogs on a screw dislocation should be given by

$$\ell_j = b\, e^{U_j/kT} \qquad (2)$$

where U_j is the jog energy and b is the Burgers vector. By plotting the log of the measured pinning point separation against $\frac{1}{T}$ the jog energy in silicon was estimated as 1.1 to 1.2 ev.

When a moving screw dislocation is pinned by jogs, the dislocation line bows-out between the pinning points. Geometrically, such a bowing-out corresponds to the piling-up of kinks of opposite sign on opposite sides of the pinning points.[23] The jogs can move forward only by climb. Thus, under applied stress τ, the glide of a bowed screw dislocation must involve both the generation and propagation of kinks and the non-conservative motion of jogs. It is necessary to distinguish which of the two is the rate-controlling process for dislocation glide.

First consider the climb of jogs. The force F acting at a jog due to the line tension Γ is given by:

$$F = 2\Gamma \cos \frac{\alpha-\theta}{2} = 2\Gamma \left[\cos \frac{\alpha}{2} \cos \frac{\theta}{2} + \sin \frac{\alpha}{2} \sin \frac{\theta}{2} \right] \qquad (3)$$

where θ is the radius of curvature of the dislocation line and α is the angle between bowed-out segments on either side of the jog. From the topographs, it was difficult to measure the angle α as a function of temperature. However, to a first approximation, it appeared that α did not vary very much with temperature. That is, the dislocation line on either side of the jogs had to bow-out to a certain critical radius of curvature, which was independent of the temperature, before the jogs would advance in the forward direction. This suggests that the jogs were moving forward without appreciable aid from thermal fluctuations. Also, the radius of curvature was not uniform along the segments between adjacent pinning points. The dislocation was more sharply curved near the jogs leaving the middle portions of the segment relatively straight. This is consistent with the idea that the dislocation advances by nucleation of kink-pairs and their subsequent slow sidewise motion towards the jogs. When a critical radius of curvature is reached on both sides of a jog due to kink pile-ups, the jog would be forced to move forward athermally. If the entire bowed-out configuration of the dislocation line were to advance a distance b per emission or absorption of a single vacancy by jogs, the work produced by the applied stress τ would be $\tau b^2 \ell_j$. For an average value of $\ell_j = 20\mu$ and $\tau = 36$ gm/mm^2, this work becomes $\sim$7 e.v. Since this is very large, the jogs could not be the rate controlling obstacles. It was concluded that in the present case, the jogs on screw dislocations did not control their glide motion; but did account for the generally irregular appearance of the

moving dislocation lines. For dislocations which are in 60° - orientation and for those portions between screw and 60° - orientation, jog motion can be conservative. This could explain the greater smoothness of dislocations in these orientations.

According to the above interpretation, the thermally activated process of dislocation motion is identified with the nucleation of pairs of kinks and their subsequent propagation along the dislocation line. The shapes of the lines observed in the present experiments varied from smoothly curved to highly irregular. If only the kink nucleation process was difficult and kink migration velocity was high, it would be expected that the dislocation lines would be straighter than was observed. Therefore, in formulating a model for glide, it is assumed that both kink-nucleation and migration are important.

The glide of dislocations over Peierls Nabarro barriers has been considered by a number of workers assuming varying mathematical models for kink nucleation and propagation. Following Dorn and Rajnak[24] kinetic equations for kink nucleation and migration can be applied to the present experiments.

Their analysis leads to an expression for the glide velocity, v, of the form:

$$v = \frac{4\nu b}{\pi} \left[\frac{\tau_p \tau b^3}{kT} \right]^{1/2} \exp \left[- \frac{E_m + E_n(\tau)}{2kT} \right] \qquad (4)$$

where ν is the atomic vibration frequency, b is the Burgers vector, τ_p is the Peierls stress, τ is the applied stress, E_m and $E_n(\tau)$ are the activation energies for kink migration and kink pair nucleation respectively. T is the absolute temperature, and K is Boltzmann's constant. The velocity-stress law can be derived from Eq. 4. E_n is a function of

applied stress. As shown by Dorn and Rajnak, the quantity E_n/E^*, where E^* is the energy required to nucleate a pair of kinks under zero stress depends only upon $\frac{\tau}{\tau_p}$. Thus, $\frac{E_n}{E^*}$ vs. $\frac{\tau}{\tau_p}$ curves are universal relationships. For very small values of $\frac{\tau}{\tau_p}$, as is the present case, their plots yield

$$E_n = E^* \left[1 - \frac{\tau}{\tau_p}\right]^{3/2} \tag{5}$$

It can be seen from Eq. (4) that a plot of (ln v + 1/2 ln kT) vs. $(\frac{1}{T})$ will yield a pre-exponential term involving τ_p. By making such a plot for screw dislocations the pre-exponential term was found to be 8.8×10^2 cm(ev)$\frac{1}{2}$/sec. By equating this to the pre-exponential term of equation (5) one obtains $\tau_p = 1.76 \times 10^{10}$ dynes/cm^2. By itself this value has no significance, since τ_p will depend upon the assumed shape of the potential. However, this result shows that the term $\frac{\tau}{\tau_p}$ is extremely small for stresses of the order of 40 gm/mm^2. Therefore, the exponential

$$\exp\left[-E_n(\tau)/kT\right] = \exp\left[\frac{-E^*(1 - \frac{\tau}{\tau_p})^{3/2}}{kT}\right] \tag{6}$$

can be approximated, by Taylor series and power series expansion, as

$$\exp\left[\frac{-E^*(1 - \frac{\tau}{\tau_i})^{3/2}}{kT}\right] \cong \frac{3}{2}\left(\frac{\tau}{\tau_p}\right)\exp\left[-E^*/kT\right] \tag{7}$$

Hence, for small applied stresses, the velocity Eq. 4 becomes

$$v = \frac{4\nu b}{\pi}\left[\frac{\tau_p\, \tau b^3}{kT}\right]^{1/2}\left[\frac{3}{2}\,\frac{\tau}{\tau_p}\right]^{3/2}\exp\left[-\frac{E^* + E_m}{2kT}\right] \tag{8}$$

This equation shows that the velocity should be proportional to τ^2, as has been observed for silicon and germanium by previous workers.

ACKNOWLEDGEMENTS

The authors are deeply grateful to Professor John Dorn for several stimulating discussions and Dr. Bertrand Escaig for many helpful comments. This work was done under the auspices of the United States Atomic Energy Commission through the Inorganic Materials Research Division of the Lawrence Radiation Laboratory.

TABLE I

Dislocation No.	Velocity in cm/sec X 10^{-5}	Remarks
Screw Segments		
1	1.07	wavy; fairly uniform motion
2	2.14	straight; uniform motion, becomes wavy
3	1.00	straight; not isolated, becomes curved
4	1.34	straight; uniform motion, a portion is stuck
5	1.20	straight; uniform motion, becomes wavy
6	1.07	straight, non-uniform motion, becomes curved
7	1.90, 1.75	" " " " " "
8	1.15	not isolated, interacted by other dislocations in the group
9	2.27	straight ahead of a pile-up
10	2.41	" " " " " "
11	0.1	curved, resists motion.
60°-segments		
13	4.91	straight, moves uniformly becomes smoothly curved
14	4.80	straight, moves uniformly fairly retains straightness
15	3.75	straight, moves uniformly fairly retains straightness
16	3.80	straight, moves uniformly fairly retains straightness
17	4.53	smoothly curved, fairly uniform motion, retains shape
18	4.05	highly irregular motion, becomes curved
19	4.42	fairly uniform motion
20	3.50	irregular motion, not isolated, ahead of a pile-up
21	5.15	smoothly curved, well isolated

TABLE II

Dislocation No.	Velocity in cm/sec X 10^{-5}	Remarks
Screw Segments		
1	2.14	straight, fairly uniform motion, becomes wavy
2	2.60	straight, ahead of a pile-up
3	1.36	piece wise straight, irregular motion
4,4'	3.21	straight, non-uniform motion, becomes irregular
5	2.91	straight, non-uniform motion, becomes irregular
6,6'	2.94, 3.3	straight, non-uniform motion, becomes irregular
7,7'	2.43	straight, non-uniform motion, becomes irregular
8	1.09	straight, non-uniform motion, becomes irregular
10	1.61	straight, fairly uniform motion, becomes curved
13	3.10	not isolated, ahead of a pile-up
60°- Segments		
1	8.0	straight, becomes smoothly curved
2	7.48	curved, non-uniform motion
4,4'	6.14, 6.95	smoothly curved, uniform motion
5	5.73	smoothly curved, uniform motion
6	3.21	smoothly curved, uniform motion
9	9.35, (1.07×10^{-4})	non-uniform motion
13, 14	9.4 (1.1×10^{-4})	straight ahead of a pile-up, retains its shape

REFERENCES

1. W. G. Johnston and J. J. Gilman, J. Appl. Phys. 30, 129 (1959).
2. D. F. Stein and J. R. Low, J. Appl. Phys. 31, 362 (1960).
3. A. R. Chaudhuri, J. R. Patel and L. G. Rubin, J. Appl. Phys. 33, 273b (1962).
4. M. N. Kabler Phys. Rev. 131, 54 (1963).
5. P. Haasen, Disc. Faraday Soc. 38, 191 (1964).
6. K. Marukawa, J. Phys. Soc. of Japan, 22, No. 2, 499 (1967).
7. H. W. Schadler, Acta Met. 12, 861 (1964).
8. R. W. Rhode and C. H. Pitt, J. Appl. Phys. 38, 876 (1967).
9. W. F. Greenman, T. Vreeland, Jr. and D. S. Wood, J. Appl. Phys. 38 3595 (1967).
10. H. L. Prekel and H. Conrad, pp. 131, Dislocation Dynamics, edited by A. R. Rosenfield, Y. T. Hahn, A. L. Bement, Jr., R. I. Jaffee, McGraw-Hill.
11. F. W. Young, Jr., and F. A. Sherrill, Can. J. Phys. 45, 757 (1967).
12. P. Petroff and J. Washburn, J. Appl. Phys. 37, 4987 (1966).
13. Theory of Crystal Dislocations by F. R. N. Nabarro, Clarendon Press (1967).
14. F. R. N. Nabarro, Z. S. Basinski and D. B. Holt, Adv. in Phys. 13 193 (1964).
15. E. S. Meieran and K. E. Lemons, Adv. in X-ray Analysis, 8, 48 (1964).
16. V. C. Kannan, Ph.D. thesis, University of California, Berkeley (Jan. 1969).
17. J. Washburn, Electron Microscopy and the Strength of Crystals, G. Thomas and J. Washburn, editors, Interscience Publ., New York (1963), Chapter 6.

18. Y. Yukimoto, Jap. J. Appl. Phys. 7, 348 (1968).

19. W. G. Johnston, J. Appl. Phys. 33, 2050 (1962).

20. H. Alexander and P. Haasen Can. J. Phys. 45, 1209 (1967).

21. J. R. Low and A. M. Turkalo, Acta. Met. 10, 215 (1962).

22. J. Friedel, Dislocations, Addison-Wesley Pub. (1964).

23. A. D. Brailsford, Phys. Rev. 122, 778 (1961).

24. J. E. Dorn and S. Rajnak, Transaction of AIME 230, 1052 (1964).

FIGURE CAPTIONS

Fig. 1 Generation and propagation of dislocations at 1025°C induced by molybdenum indenter. The well-isolated long dislocations at A are nearly in screw orientation. The line No. 1 shows presence of pinning points along the length of the dislocation, while No. 2 is smoothly curved. Large helical loops can be seen at (B), small loops at (C) and well-developed cusps at (D).

Fig. 2 (a) A tensile specimen was cut from the crystal shown in Fig. 2 and was deformed in tension at 825°C under a stress of 200 gm/mm^2 applied along $[\bar{1}10]$. The screw dislocations ($b = \frac{a}{2}[\bar{1}01]$) were subjected to a shear stress of 88 gm/mm^2. Note that the dislocations did not move any appreciable distance (compare this topograph with Fig. 1). (b) Topograph taken after heating the sample to 950°C for 15 minutes under a load of 20 gm/mm^2 along $[1\bar{1}0]$. The dislocations at B climbed towards the surface and intersected it. (c) Deformation was continued at 900°C under a load of 380 gm/mm^2 acting along $[1\bar{1}0]$. Fresh dislocations were generated from the specimen edges. Closer observation shows that the original high-temperature dislocations still did not move.

Fig. 3 Topographs showing the dislocations generated in the sample by pulling under (a) 30 gm/mm^2 950°C for 30 minutes (b) 36 gm/mm^2 at 850°C for 30 minutes. (c) 65 gm/mm^2 at 900°C for 15 minutes. The vertical direction is along the tensile axis which makes 45° to [111] and $[\bar{1}01]$ directions.

Fig. 4 Electron micrographs of thin foils of silicon made from highly deformed samples.

Fig. 5 The position of dislocations before (a) and after (b) the tensile test at 825°C, under a resolved shear stress of 36 gm/mm^2. In (a), the isolated dislocations are labelled; and their velocities are listed in Table I.

Fig. 6 Dislocations before (a) and after (b) the tensile test at 850°C under resolved shear stress of 36 gm/mm^2. Again, in (a) the dislocations are labelled and their velocities are listed in Table II.

Fig. 7 A plot of dislocation velocities against the reciprocal of temperature for screw and for 60° dislocations under a resolved shear stress of 36 gm/mm^2. The upper dashed line is for 60° dislocations while the solid lines are for screw dislocations. Solid circles are data points for curved or wavy screw dislocations while open circles are for nearly straight ones.

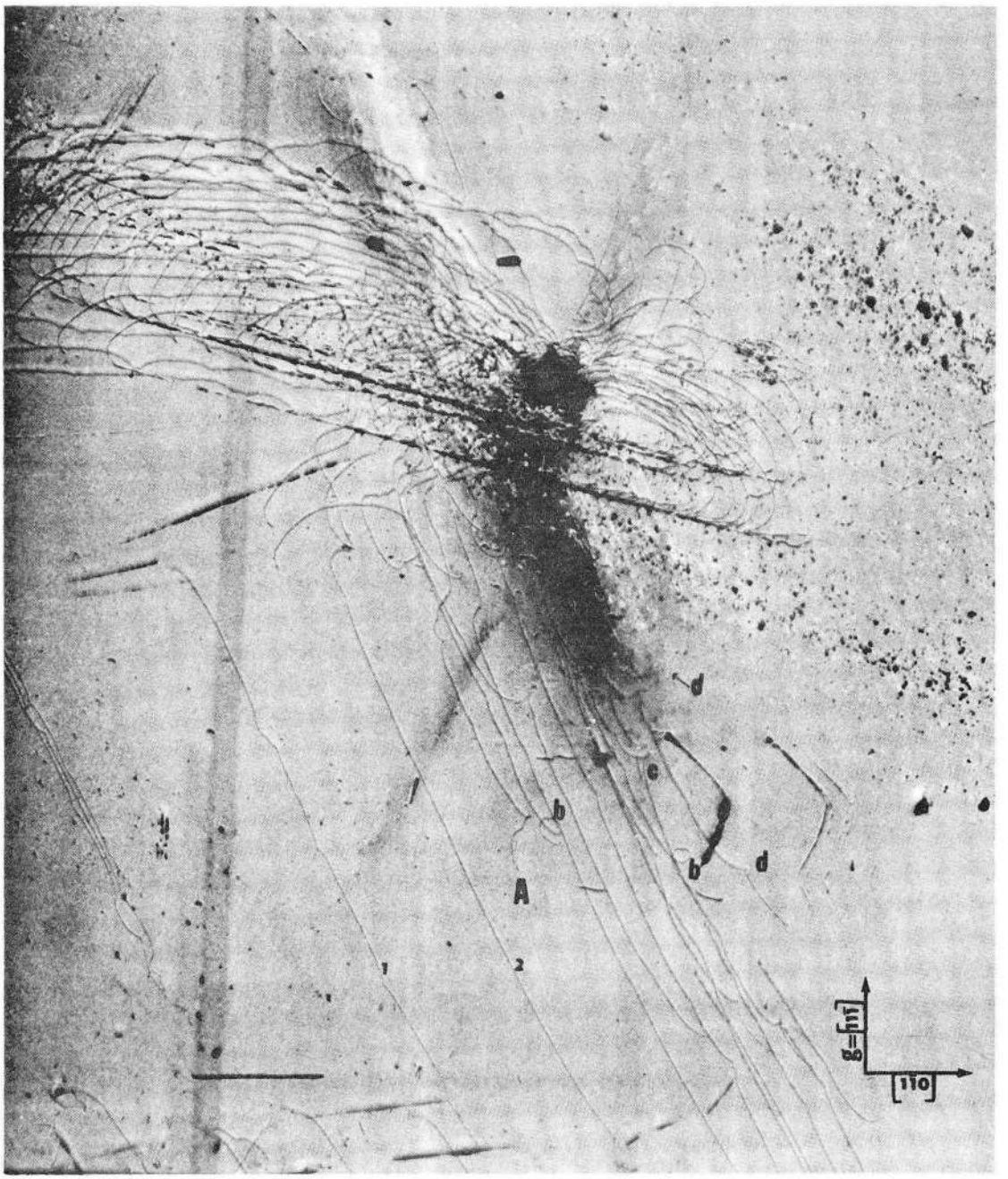

XBB 6812-7430

Fig. 1

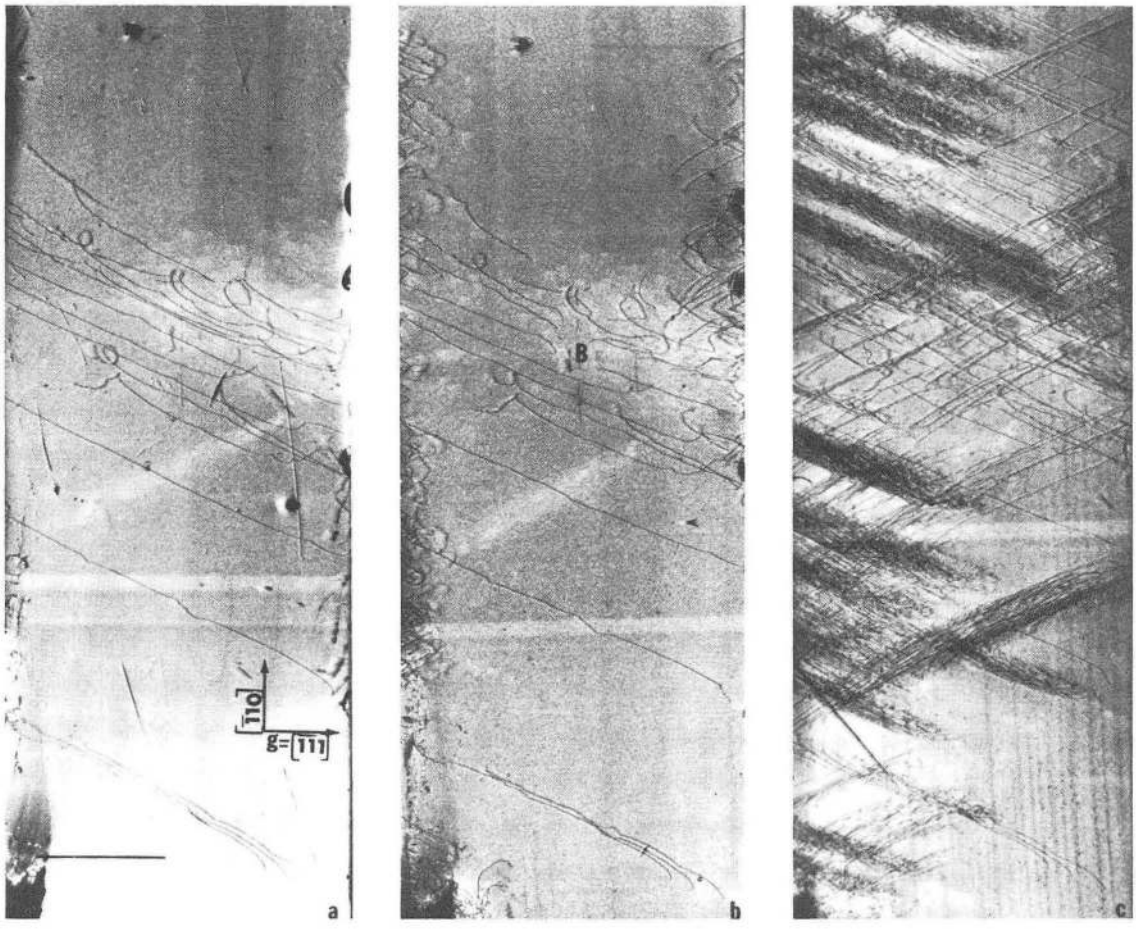

XBB 6812-7424

Fig. 2

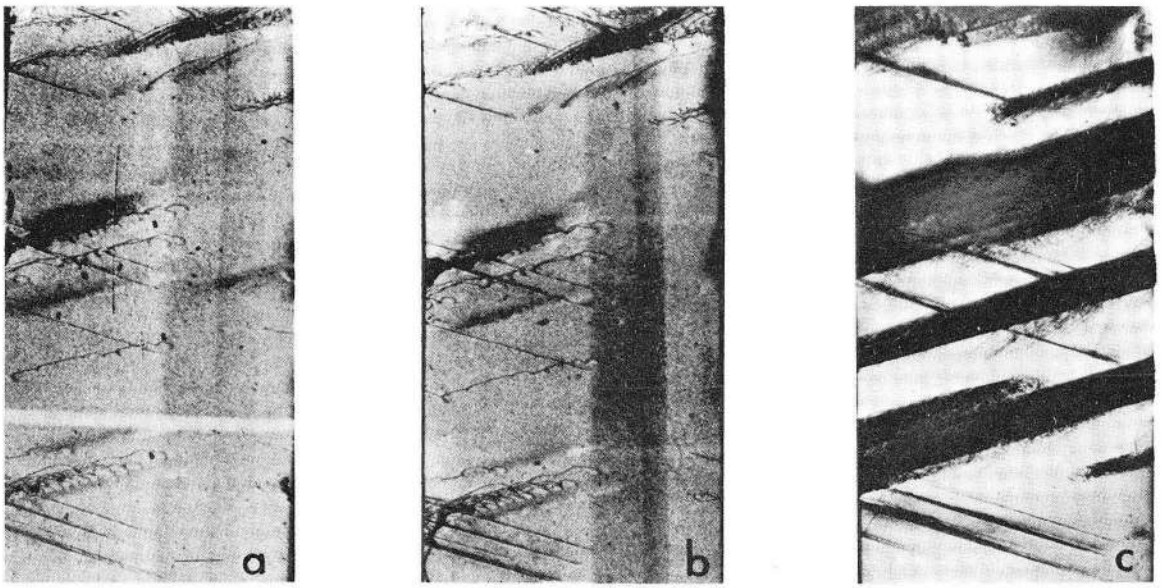

XBB 691-452-A

Fig. 3

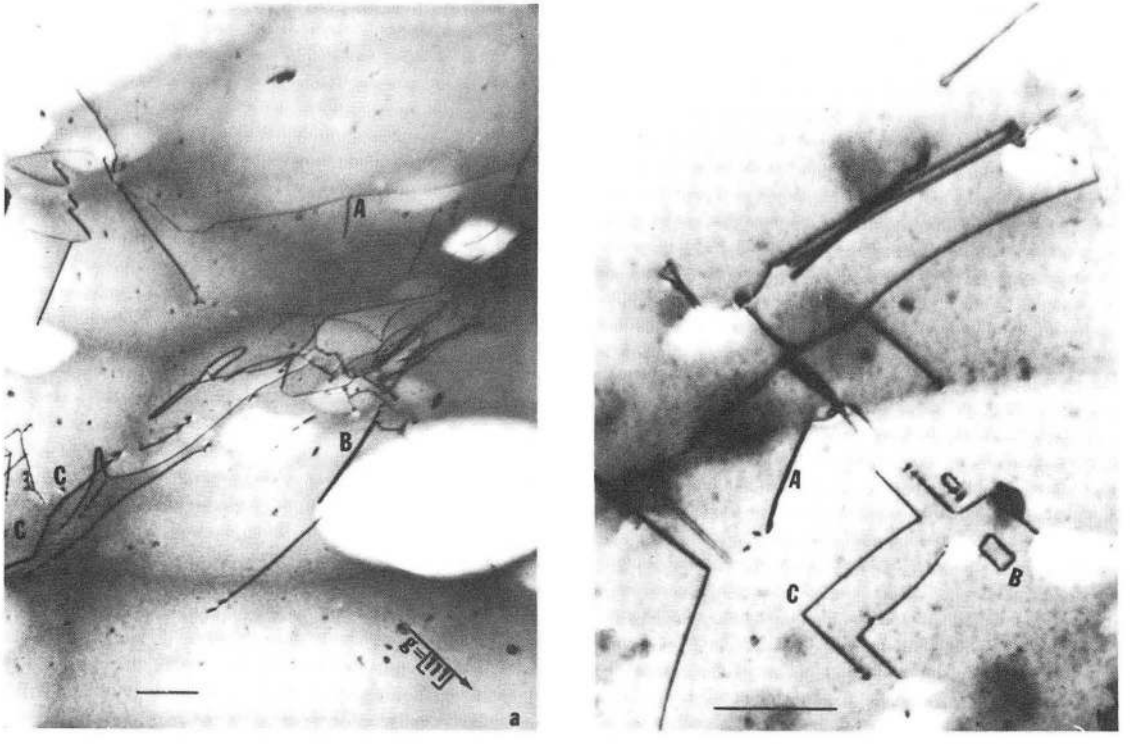

XBB 6812-7429

Fig. 4

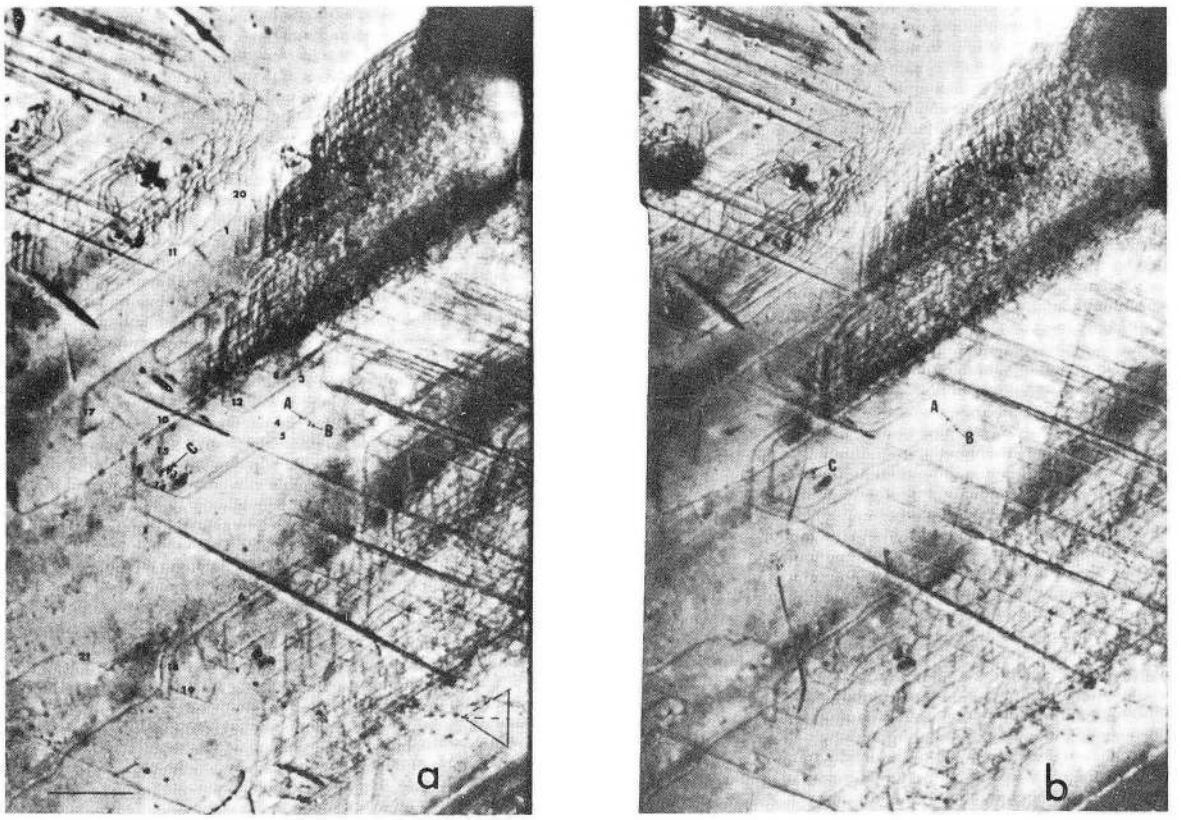

XBB 691-450-A

Fig. 5

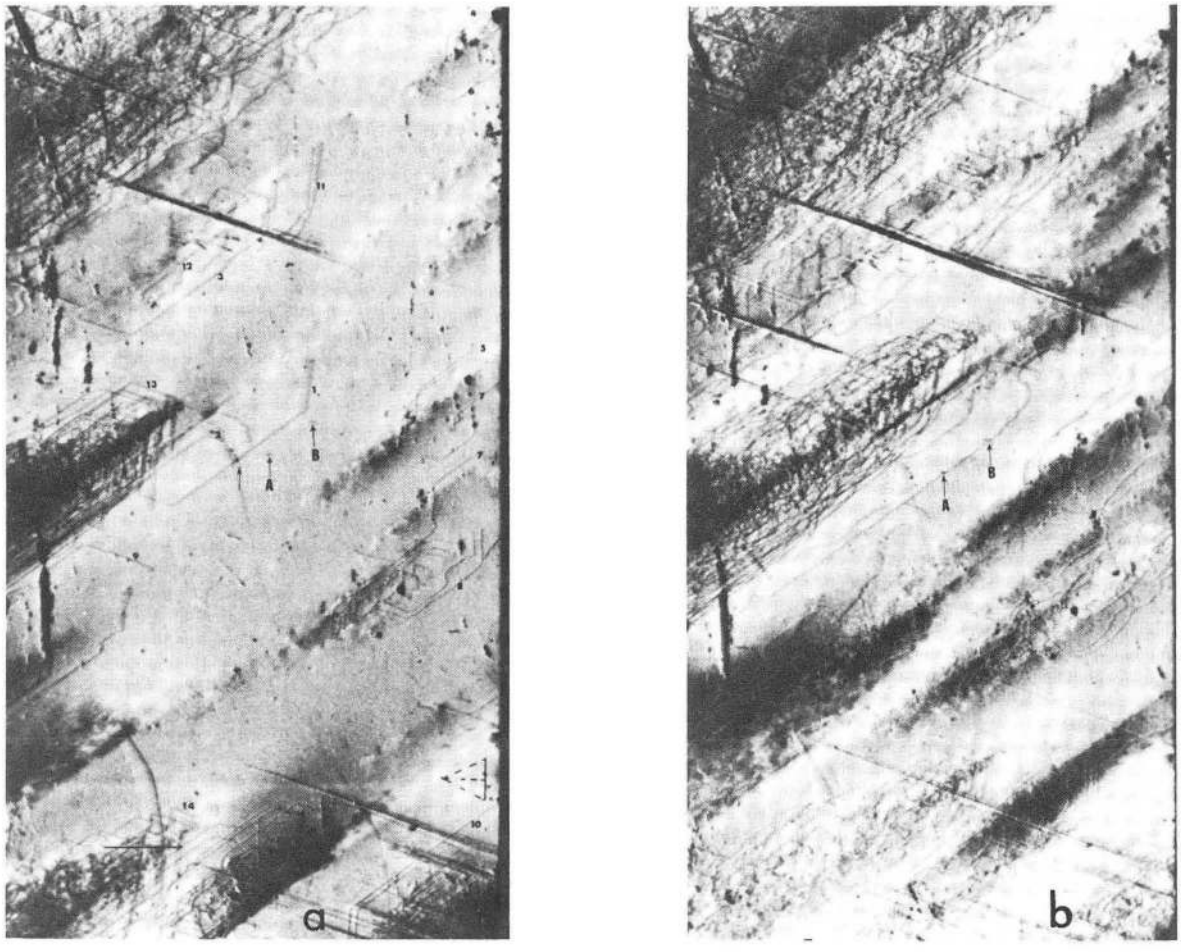

XBB 691-451-A

Fig. 6

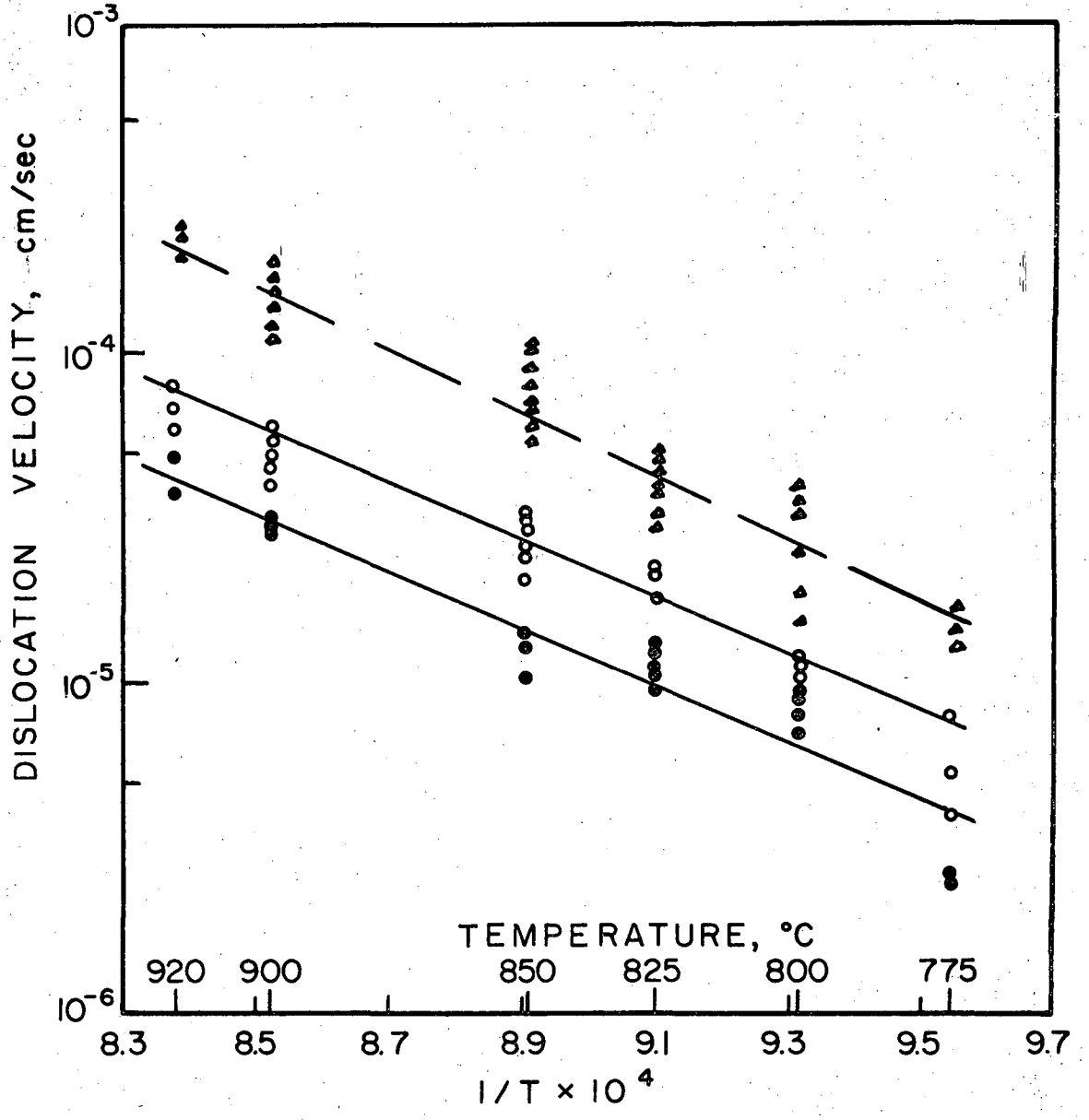

XBL 694-389

Fig. 7

LEGAL NOTICE

TECHNICAL INFORMATION DIVISION
LAWRENCE RADIATION LABORATORY
UNIVERSITY OF CALIFORNIA
BERKELEY, CALIFORNIA 94720